International Journal of Biological Macromolecules 51 (2012) 449–455

Contents lists available at SciVerse ScienceDirect

International Journal of Biological Macromolecules

journal homepage: www.elsevier.com/locate/ijbiomac

Development of an amperometric sulfite biosensor based on SO_x/PBNPs/PPY modified ITO electrode

Rachna Rawal, C.S. Pundir*

Department of Biochemistry, M D University, Rohtak 124001, Haryana, India

ARTICLE INFO

Article history:
Received 31 January 2012
Received in revised form 9 March 2012
Accepted 7 June 2012
Available online 15 June 2012

Keywords:
Sulfite
Sulfite oxidase
Amperometric
Sulfite biosensor
Prussian blue nanoparticles
Polypyrrole

ABSTRACT

A sulfite oxidase (SO_x) (EC 1.8.3.1) purified from *Syzygium cumini* leaves was immobilized onto prussian blue nanoparticles/polypyrrole composite (PBNPs/PPY) electrodeposited onto the surface of indium tin oxide (ITO) electrode. An amperometric sulfite biosensor was fabricated using SO_x/PBNPs/PPY/ITO electrode as working electrode, Ag/AgCl as standard and Pt wire as auxiliary electrode connected through a potentiostat. The working electrode was characterized by Fourier transform infrared (FTIR) spectroscopy, cyclic voltammetry (CV), scanning electron microscopy (SEM) and electrochemical impedance spectroscopy (EIS) before and after immobilization of SO_x. The biosensor showed optimum response within 2 s, when operated at 20 mV s^{-1} in 0.1 M Tris–HCl buffer, pH 8.5 and at 35 °C. Linear range and minimum detection limit were 0.5–1000 μM and 0.12 μM (S/N = 3) respectively. There was good correlation (r = 0.99) between red wine samples sulfite value by standard DTNB method and the present method. The sensor was evaluated with 97% recovery of added sulfite in red wine samples and 2.2% and 4.3% within and between batch coefficients of variation respectively. The sensor was employed for determination of sulfite level in red and white wine samples. The enzyme electrode was used 200 times over a period of 3 months when stored at 4 °C.

1. Introduction

Determination of sulfite is important; particularly from biological and industrial point of view, as it is widely used as a preservative and antioxidant in food, beverages and pharmaceuticals. Sulfite oxidase (SO_x) (EC 1.8.3.1) is a metallo-enzyme, which utilizes a molybdopterin as a cofactor and belongs to a superfamily of enzymes including dimethylsulphoxide (DMSO) reductase, xanthine oxidase and nitrite reductase. The human SO_x is located in mitochondrial intermembranous space and involved in the transfer of electrons from sulfites into the electron transfer chain (ETC) via cytochrome c. Studies have shown that human serum contains sulfite concentration in range of 0–10 μM [1,2]. Food and Drug Administration (FDA), USA, has instrumented warning labels on any food containing more than 10 mg/kg or beverages containing more than 10 mg/L of sulfite [3,4]. The catabolism of sulfur containing amino acids, methionine and cysteine contributes to the bulk of the sulfite load in the body. The quantitative determination of sulfite in different types of samples has been reported employing a range of analytical techniques such as iodimetry [5], colorimetric/DTNB method [6], spectrophotometry [7–10], anodic stripping voltammetry [11], reciprocal oscillographic chronopotentiometry [12], ion chromatography [13], enthalpimetry [14], chemiluminescence [15,16], gravimetry [17], ion selective electrode [18,19], gas chromatography [20] and HPLC [21]. However, these analytical techniques are labor-intensive, time consuming sample and reagent preparations and lack precision/sensitivity. Hence development of an enzyme biosensor for detection of sulfite is of considerable interest, since it would allow fast, selective and accurate determination of sulfite, without the need for significant sample preparation. A number of sulfite biosensors have been reported viz. glassy carbon electrode coated with thin mercury film [22], polytyramine-platinized glassy carbon electrode [12], polyaniline-sulfonic acid [23], polypyrrole films [24], on conducting polyaniline film [25], self-assembled monolayer of 11-mercaptoundecanol (MU) cast on a gold electrode [26], on gold nanoparticles/chitosan/multiwalled carbon nanotube/polyaniline modified gold electrode [27]. The disadvantages of these reported biosensors include limited detection limit due to poor electron flow and low storage stability of the working electrode. Polypyrrole (PPY) is useful in construction of biosensor, because of its high conductivity, good environmental stability and large variety of applications. Composites containing PPY and any inorganic nanoparticles such as AgNPs, AuNPs, CuSNPs and prussian blue nanoparticles (PBNPs) have been synthesized. Among those inorganic materials, PBNPs have received much attention and play many important roles in the fields of magnetic molecules,

* Corresponding author. Tel.: +91 9416492413.
E-mail addresses: pundircs@rediffmail.com, pundircs@gmail.com, pundircs@yahoo.com (C.S. Pundir).

0141-8130/$ – see front matter © 2012 Elsevier B.V. All rights reserved.
http://dx.doi.org/10.1016/j.ijbiomac.2012.06.008

electrochromic devices and rechargeable batteries owing to their interesting electrochemical, photophysical, and magnetic properties [28,29]. PBNPs–PPY composite film is expected to exhibit many advantages like high activity, excellent electrochemical activity and selectivity in detection of H_2O_2 [30–32]. The present work describes the construction of sulfite biosensor based on *Syzygium cumini* leaf SO_x immobilized on PBNPs–PPY electrodeposited onto ITO electrode and its application for measurement of sulfite in red and white wine samples

2. Experimental

2.1. Chemicals

Sephadex G-100 and DEAE-Sephacel from Sigma–Aldrich, St. Louis, USA, sodium sulfite, potassium ferricyanide, ferric chloride and pyrrole from Sisco Research Laboratory (SRL), Mumbai, India were used. All other chemicals used were of Analytical Reagent (AR) grade. The mature leaves of *S. cumini* (Jamun) plants growing on road side of new campus of M.D. University, Rohtak were collected, brought to the laboratory immediately in a ice bath, washed thoroughly with Double distilled water (DW), dried between folds of filter paper and stored at −20 °C until use. Indium tin oxide coated glass plate (ITO) (2 cm × 1 cm) was a gift from Metrohm India Limited. Different brands of red and white wines were purchased from market of different states of India. DW was used throughout the experiments.

2.2. Extraction and purification of SO_x from leaves of S. cumini

SO_x from frozen jamun leaves was extracted as described [33], with modification by homogenizing leaves with cold 0.1 M Tris–HCl (pH 8.0) in 3:1 ratio (w/v) in a chilled pestle and mortar. The extract was filtered through a muslin cloth and the filtrate was centrifuged at 10,000 × *g* for 30 min at 4 °C. The pellet was discarded and supernatant was collected and treated as crude enzyme. It was tested for sulfite oxidase activity and protein concentration by Lowry method. Crude enzyme was purified as described using a combination of 0–80% ammonium sulfate precipitation, gel filtration on Sephadex G-100 and ion-exchange chromatography on DEAE Sephacel using linear gradient of KCl (0.1–0.6 M) [33]. Finally, the enzyme was purified by 57-fold with 19.5% yield.

2.3. Assay of SO_x

The assay of SO_x was carried out as described with modifications and based on quantification of H_2O_2 generated from sulfite, using a color reaction consisting of 4-aminophenazone, phenol and peroxidase as chromogenic system [34]. The reaction mixture containing 1.8 mL of 0.1 M Tris–HCl buffer pH 8.5, and 0.1 mL enzyme preparation was preincubated at 35 °C for 5 min. The reaction was started by adding 0.1 mL of 0.4 mM sodium sulfite. After incubation at 35 °C for 10 min in dark, 1.0 mL color reagent was added and kept at room temperature for 15 min. to develop the color. A_{520} was read and H_2O_2 content generated during the reaction was interpolated from a standard curve between H_2O_2 conc. and A_{520} prepared in 0.1 M Tris–HCl buffer, pH 8.5.

One unit of enzyme is defined as amount of enzyme required to catalyze the formation of 1.0 nmol of H_2O_2 from oxidation of sulfite per min under standard assay conditions.

Preparation of color reagent: The color reagent was prepared according to the method of Bais et al. and consisted of 50 mg 4-aminophenazone, 100 mg solid phenol and 1 mg horseradish peroxidase per 100 mL of 0.4 M sodium phosphate buffer, pH 7.0 [35]. It was stored in amber colored bottle at 4 °C and discarded after one week.

2.4. Preparation of prussian blue nanoparticles (PBNPs)

PBNPs were prepared by mixing equimolar amount of $FeCl_3$ and $K_4[Fe(CN)_6]$ aqueous solutions. 2 mL of $FeCl_3$ (2 mM) solution was poured slowly drop wise into 2 mL of $K_4[Fe(CN_6]$ (2 mM) solution under vigorous stirring. A blue coloured solution was gradually formed indicating the formation of PBNPs. Then PBNPs were subjected to sonication for about 30 min [36].

2.5. Preparation of enzyme electrode (SO_x/PBNPs/PPY/ITO electrode)

Firstly, the ITO coated glass plate was washed with DW and dried at room temperature. Then, ITO coated glass electrode was immersed into 0.1 M phosphate buffer (PB) solution (pH 7.0) containing 0.2 M pyrrole and 0.1 M KCl and subjected to cyclic voltammetry (CV) in a potential range, −0.2 to (+0.6 V) (vs Ag/AgCl) for electro-polymerization and deposition of polypyrrole on the surface of electrode (PPY/ITO). The thickness of the PPY film was controlled by the scanning times (12–15 times) in electrodeposition. Then, PBNPs were electrodeposited onto PPY/ITO electrode by immersing it into a mixture of 20 mL of 0.1 M KCl and 5 mL of PBNPs colloidal solution and applying same potential as above. After rinsing with DW, PBNPs/PPY/ITO electrode was dried in air.

The purified SO_x was immobilized onto the surface of PBNPs/PPY/ITO electrode through adsorption by layering its 100 μL solution in PB pH 7.0 containing 3.0 μg protein and keeping it undisturbed for about 12 h at 4 °C. ITO coated glass plate was finally washed with 0.1 M Tris–HCl buffer (pH 8.5) to remove unbound enzyme. The protein concentration in remaining solution and wash out solution were determined.

2.6. Characterization of enzyme electrode

The modified ITO electrode, at different stages of its construction was characterized by scanning electron microscopic (SEM) images in Scanning Electron Microscope (Make: Joel Japan, Model: JSM-6510, at Advanced Instrumentation Research Facility, JNU, New Delhi). Fourier transform infrared (FTIR) spectra in FTIR spectometer (Make: Thermoelectron, USA, Model: iS10) and cyclic voltammetric and electrochemical impedance spectroscopic (EIS) studies on potenitostat/galvanostat (Make: Autolab, Eco Chemie BV, Netherlands, Model: AUT83785 with the GPES 4.9 software) with three electrode system, SO_x/PBNPs/PPY/ITO electrode as the working electrode, a Pt wire as the auxiliary electrode and an Ag/AgCl (saturated 3 M KCl) electrode as the reference electrode. The EIS measurements were carried out in 1 mM $K_3[Fe(CN)_6]$ in the 0.1 M PB pH 7.0 at ambient temperature, at the polarization potential of 0.2 V (vs Ag/AgCl) in the frequency range 0.1–10^4 Hz and with the amplitude of 10 mV. The resulting enzyme electrode (SO_x/PBNPs/PPY/ITO electrode) was stored in refrigerator at 4 °C, when not in use. To record FTIR spectra of hybrid material deposited onto ITO electrode, it was scrapped off the ITO electrode, mixed with dried KBr and its pellet was formed by hydraulic pellet press. Then this pellet was kept into the socket of the FTIR spectrometer and its spectrum was recorded.

2.7. Response measurement of SO_x/PBNPs/PPY/ITO electrode

Cyclic voltammetric measurements were carried out in a three electrode cell containing reaction mixture 20 mL KCl as electrolyte (0.1 M), 5 mL Tris–HCl buffer (0.1 M, pH 8.5) and 0.1 mL of sulfite

(0.4 mM). Current (μA) was measured applying CV in the potential range between −0.2 and +0.6 V (vs Ag/AgCl).

2.8. Optimization of SO_x/PBNPs/PPY/ITO electrode

To determine the optimum working conditions of the enzyme electrode, the pH of reaction buffer (0.1 M) was varied from pH 5.0 to 10.5 at an interval of pH 0.5 using sodium phosphate buffer between pH 5.0 and 7.0 and Tris–HCl buffer between pH 7.5 and 10.5. Similarly, to determine optimum temperature, the reaction mixture was incubated at 10–50 °C at an interval of 5 °C. Optimum response time was studied by measuring current between 0 and 12 s at an interval of 2 s. To study the effect of substrate concentration, different sulfite concentrations were used, in the range from 0.5 to 1000 μM. The amperometric response was also measured in the presence of potential interfering compounds found such as glucose, fructose, ascorbic acid, cysteine, ethanol and citric acid in the concentration range generally found in wines.

2.9. Evaluation

The following criteria were studied to evaluate the analytic performance of the biosensor e.g. linearity, analytical recovery, detection limit, precision and correlation. Analytical recovery was studied using red wine samples with two different standard concentrations (20 and 40 μM) of sulfite. The sulfite concentrations in the red wine samples were determined before and after adding these standard concentrations by the present biosensor, to calculate % recovery of added sulfite concentrations. To test the reproducibility and reliability of the present biosensor, sulfite level in six alcoholic beverage samples was measured five times on single day (within batch) and five times again after their storage at −20 °C for one week (between batch). To study the correlation, the sulfite level was measured in 15 brands of red wine samples by the standard 5,5′-Dithio-bis(2-nitrobenzoic acid (DTNB) method and the present method and their correlation was studied by using regression equation. The wine sample analysis by standard DTNB method [6] was carried out follow: A known amount of red wine sample solution was placed in a 10 mL volumetric tube and diluted with water to 8 mL. Then 1 mL of DTNB solution (0.060 g of DTNB per 100 mL of 10% ethanol) was added and the solution was diluted to the 10-mL mark line with water. The absorbance was measured at 412 nm with deionized water as the reference after 5 min reaction at room temperature. To examine the long-term storage stability, the activity of enzyme electrode was tested up to 3 months at an interval of 1 week, when stored at 4 °C. To reuse the enzyme electrode, it was washed 3–4 times with reaction buffer before its use in next assay.

2.10. Amperometric measurement of sulfite in red and white wines

We analyzed both red and white wine samples of freshly opened bottles after their storage for 2 weeks at room temp. Sulfite level in red and white wine samples was measured by the present biosensor in the same manner as described above for its response measurement under its optimal working conditions except that sulfite was replaced by the sample. The current (μA) was recorded and the amount of sulfite was interpolated from standard curve between sulfite concentrations and current (μA) prepared under optimal working conditions.

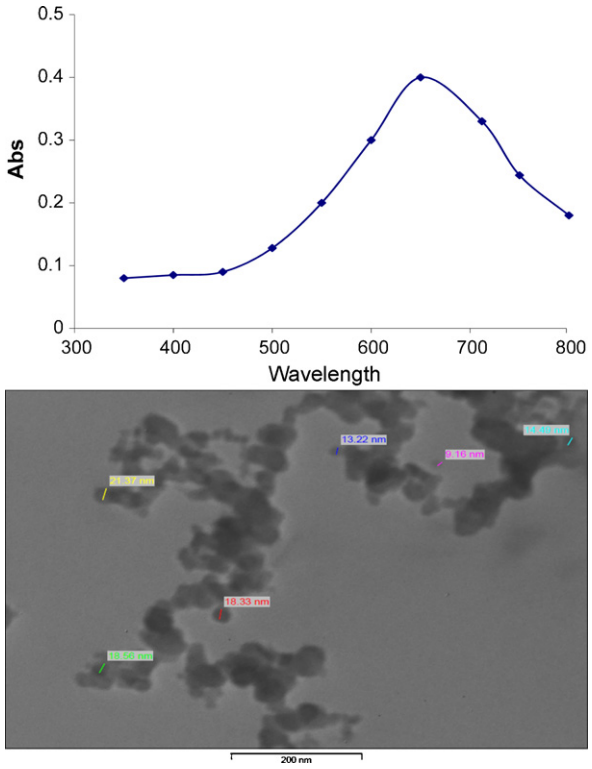

Fig. 1. (a) UV–vis absorption spectra of PBNPs and (b) transmission electron microscopic (TEM) image of PBNPs.

3. Results and discussion

3.1. Characterization of PBNPs

The characterization of PBNPs was carried out by UV–vis absorption spectra (Fig. 1a) and TEM image (Fig. 1b). The UV–vis spectrum of the resulting solution showed a broad band with λ_{max} at 650 nm, which is consistent with an intermetal charge transfer band from Fe^{2+} to Fe^{3+} in Prussian blue. TEM image of prepared PBNPs showed their spherical shape with different diameter in the range, 9–22 nm revealing their different sizes but not shape. The apparent variations in the shape of PBNPs could be possible due to aggregation of nanoparticles.

3.2. Construction of SO_x/PBNPs/PPY/ITO electrode

A sulfite oxidase electrode was prepared by first electrodepositing PPY and then PBNPs onto ITO coated glass plate followed by layering of enzyme (purified SO_x) onto the surface of this modified electrode (PBNPs/PPY/ITO) for its physiosorption. Scheme 1 summarizes reactions involved in construction of sulfite oxidase electrode. A method is described for construction of an amperometric sulfite biosensor using this enzyme electrode (SO_x/PBNPs/PPY/ITO) as working electrode, Ag/AgCl as reference and Pt wire as auxillary electrode connected through potentiostat.

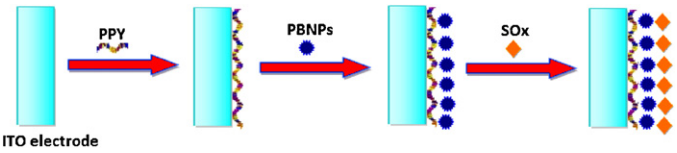

Scheme 1. Scheme of chemical sequence of electropolymerization of onto PBNPs/PPY/ITO electrode and chemical reaction of immobilization of enzyme (sulfite oxidase) on modified electrode.

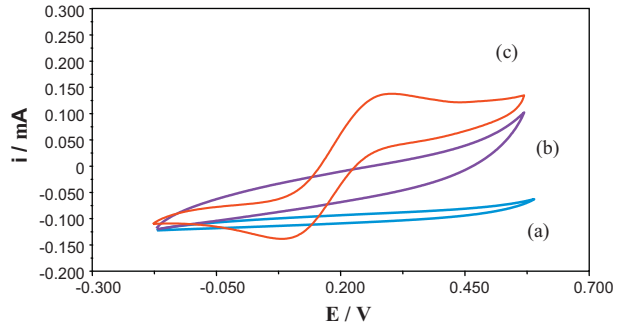

Fig. 2. Cyclic voltammetric responses of (a) bare ITO, (b) PPY/ITO electrode, (c) PBNPs/PPY/ITO electrode in 0.1 M Tris–HCl (pH 8.5). Supporting electrolyte: 0.1 M KCl solution; scan rate: 20 mV s^{-1}.

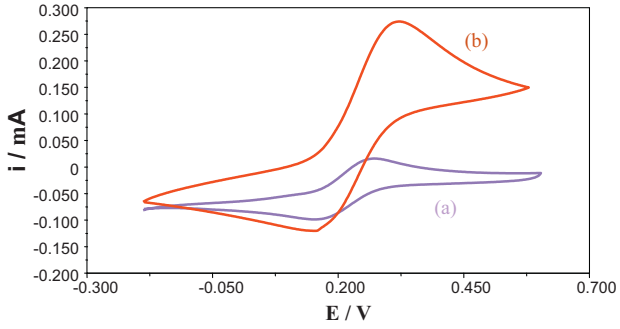

Fig. 3. SO_x/PBNPs/PPY/ITO electrode in (a) without sulfite and (b) with sulfite in 0.1 M Tris–HCl buffer (pH 8.5). Supporting electrolytes: 0.1 M KCl solution; scan rate: 20 mV s^{-1}.

Fig. 2 shows cyclic voltammograms (CV) of ITO electrode in a solution containing 0.1 M KCl solution. The bare ITO electrode (curve a) shows no redox peak. When a layer of PPY was electrodeposited over bare ITO electrode, only the current characteristic of PPY was noticed (PPY/ITO) (curve b). PBNPs modified ITO electrode (PBNPs/PPY/ITO) (curve c) showed excellent redox properties in CV. A couple of well-defined cathodic (−0.17 V) (vs Ag/AgCl) and anodic (0.32 V) (vs Ag/AgCl) peaks are revealed.

In Fig. 3 SO_x/PBNPs/PPY/ITO electrode and its cyclic voltammogram has been recorded in (a) the absence of sulfite and (b) the presence of sulfite. The oxidation peak seen at 0.32 V (vs Ag/AgCl) corresponding to the oxidation of H_2O_2 arisen due to the enzymatic reaction between SO_x and sulfite (Fig. 4). The increase in the value of the oxidation current with increase in sulfite concentration resulted due to the increased concentration of H_2O_2 during enzymatic reaction. This well-defined oxidation peak (at 325 mV) indicated clearly the catalytic properties of modified electrode. Thus, for further amperometric study of SO_x/PBNPs/PPY/ITO electrode, a potential of 0.32 V was applied.

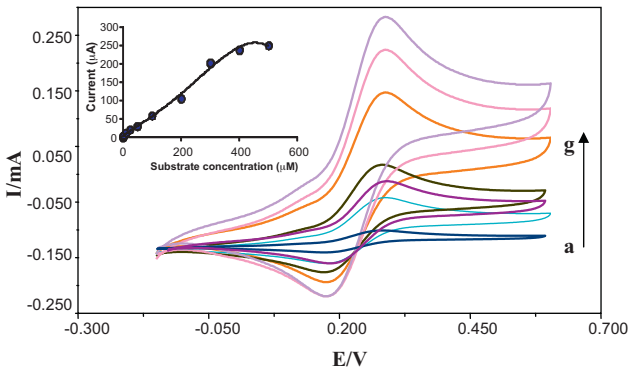

Fig. 4. Cyclic voltammograms recorded at different concentration of sulfite from (a) 0.5, (b) 100, (c) 200, (d) 400, (e) 600, (f) 800 and (g) 1000 μM; scan rate: 20 mV s^{-1}. Inset: standard curve for sulfite by sulfite biosensor based on SO_x immobilized onto PBNPs/PPY/ITO electrode.

The electrochemical reactions involved in amperometric sulfite biosensor were as follow:

$$\text{Sulfite} + O_2 + H_2O \xrightarrow{SO_x} \text{sulfate} + H_2O_2$$

$$H_2O_2 \xrightarrow{0.3\,V} 2H^+ + O_2 + 2e^-$$

$$2e^- \xrightarrow{PBNPs/PPY} \text{ITO electrode}$$

3.3. Surface characterization by SEM

The surface morphologies of bare ITO electrode, PBNPs/PPY/ITO electrode and SO_x/PBNPs/PPY/ITO electrodes were studied by SEM (Fig. 5). Bare electrode showed homogenous surface (Fig. 5a), whereas the PBNPs/PPY/ITO electrode has uniform granular porous morphology attributed to the homogeneous dispersion of PBNPs nanoparticles in PPY network (Fig. 5b). On immobilization of SO_x, the globular structural of PBNPs/PPY changed into the regular form (Fig. 5c), due to the electrostatic interaction of PBNPs/PPY with SO_x [37]

3.4. FTIR spectra

Fig. 6 shows FTIR spectrum of PPY (curve a) with characteristic absorption bands at 1545 and 1343 cm^{-1} corresponding to the fundamental vibration of the pyrrole ring. The peaks at 1294, 1045, 763 cm^{-1} can be assigned to the =C—H— in plane vibration. FTIR spectra of PBNPs/PPY (curve b) shows absorption bands at 1545 and 1343 cm^{-1} for typical pyrrole ring vibration and for PBNPs characteristic peak at 497 cm^{-1} was observed due to the formation of Fe^{2+}—C≡N—Fe^{3+}. They indicate the presence of PBNPs.

3.5. Electrochemical impedance measurements

EIS studies provide useful information on impedance changes of the electrode surface during the fabrication process and were carried out to investigate immobilization of enzyme onto PBNP/PPY/ITO electrode. The diameter of the semicircle portion at higher frequencies of the Nyquist plot was equal to the charge transfer resistance (RCT), which controls the electron transfer kinetics of the redox probe at the electrode interface. Meanwhile, the linear part at lower frequencies corresponds to the diffusion process [38]. The Nyquist plot (Fig. 7) displays EIS studies of (a) PPY/ITO electrode (b) PBNPs/PPY/ITO electrode (c) SO_x/PBNPs/PPY/ITO electrode respectively, in 0.1 M PBS pH 7.0 containing 1 mM $K_3Fe(CN)_6/K_4Fe(CN)_6$ (1:1) as a redox probe. It was observed that the RCT of PBNPs/PPY/ITO electrode was 1800 Ω (curve b), which is lower than PPY/ITO electrode (2500 Ω) (curve a), revealing its decreased resistance and high electron transfer efficiency. However, the R_{CT} of SO_x/PBNP/PPY/ITO electrode (3500 Ω) (curve c) increased compared with that of PBNP/PPY/ITO electrode. This increase in R_{CT} can be attributed to the fact that most biological molecules, including enzymes, are poor electrical conductors at low frequencies and cause hindrance to electron transfer. These results also indicate the binding of enzyme (SO_x) onto PBNP/PPY/ITO composite.

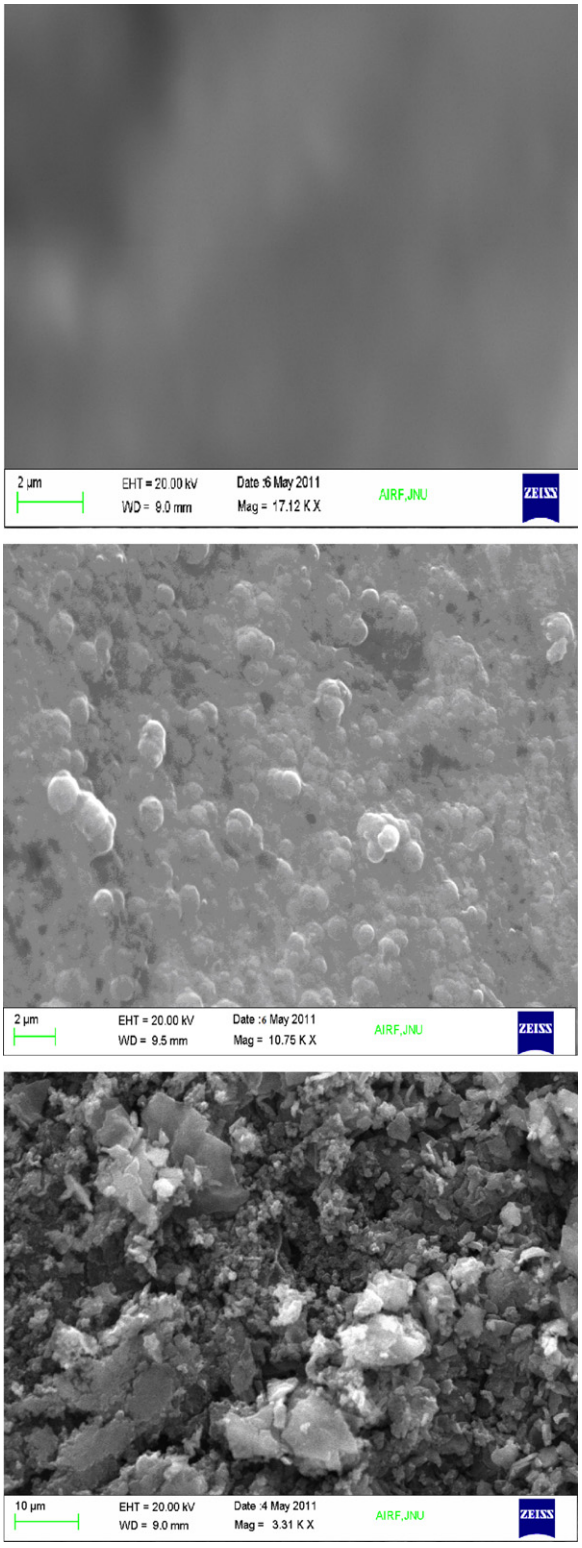

Fig. 5. SEM image of (a) bare ITO electrode, (b) PBNPs/ITO electrode and (c) SO_x/PBNPs/PPY/ITO electrode.

3.6. Optimization of the biosensor (SO_x/PBNPs/PPY/ITO electrode)

The biosensor showed optimum response (current in µA) at pH 8.5, which is higher than that for SO_x bound to screen printed strip modified carbon electrode (pH 7.5) [39], glassy carbon coated thin mercury film (pH 7.0) [22], polypyrrole film (pH 7.0) [24], comparable to that of SO_x bound to polyaniline on aluminum surface

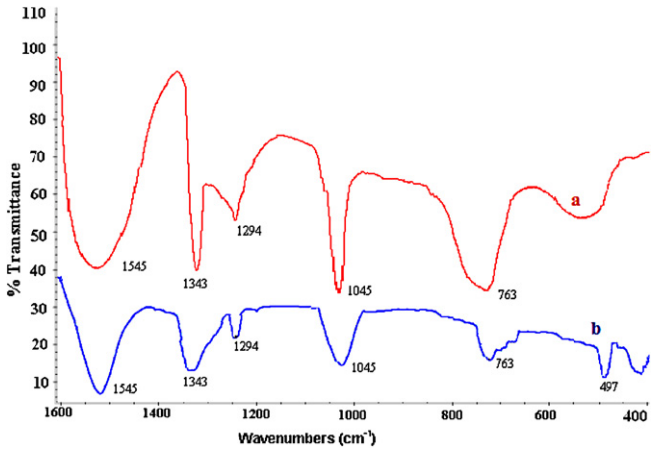

Fig. 6. FTIR spectra of (a) PPY/ITO electrode and (b) PBNPs/PPY/ITO electrode.

(8.5) [40]. Therefore, a pH of 8.5 was used in further experiments (Supplementary Fig. 1(a)). The optimum temperature of biosensor was 35 °C (Supplementary Fig. 1(b)) which is lower than that for glassy carbon coated thin mercury film (40 °C) [22]. The effect of the scan rate from 10 to 100 mV s^{-1} on the biosensor response using 0.4 mM sodium sulfite in 0.1 M Tris–HCl buffer solution (pH 8.5) was also investigated. A potential scan rate of 20 mV s^{-1} was selected, since with these experimental conditions, the highest analytical signal and very good cyclic voltammogram profiles were obtained. The response of the present electrode system in relation to the change in sodium sulfite concentration was found linear in the range of 0.5–1000 µM. Fig. 4 shows cyclic voltammogram response of electrode for different concentration of sulfite (0.5–1000 µM).

3.7. Evaluation of the performance of the biosensor

There was a linear relationship between current (µA) and sulfite concentration ranging from 0.5 to 1000 µM which is a better linear range than those of earlier biosensors based on SO_x immobilized onto polytyramine-platinized glassy carbon electrode (2–300 µM) [12], polyaniline-sulfonic acid (1–60 µM) [23] and polypyrrole films (0.9–400 µM) [24]. The detection limit of the present sensor was 0.12 µM (S/N = 3), which is lower than that for enzyme immobilized onto SOx/AuNP's/CHIT/cMWCNT/PANI/Au electrode (0.5 µM) [27], polytyramine-platinized glassy carbon electrode (2 µM) [12], polyaniline-sulfonic acid (1 µM) [23], polypyrrole films (0.9 µM) [24] and Teflon membrane (200 µM) [41]. The analytical recoveries of added sulfite in red wine samples (20 µM and 40 µM) were 96.40–97.26%, respectively, demonstrating the satisfactory accuracy of the present method. Within and between coefficients

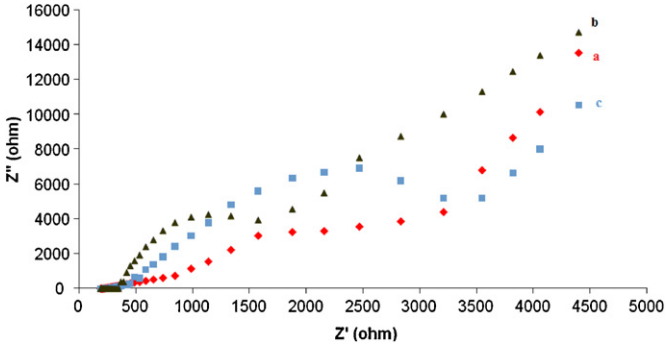

Fig. 7. Impedance spectra of (a) PPY/ITO, (b) PBNPS/PPY/ITO electrode and (c) SO_x/PBNPs/PPY/ITO electrode.

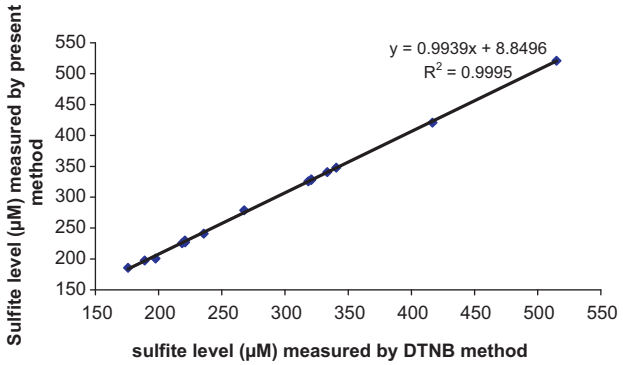

Fig. 8. Correlation between sulfite values as determined by standard DTNB method (x-axis) and present biosensor method employing SO_x/PBNPS/PPY/ITO electrode (y-axis).

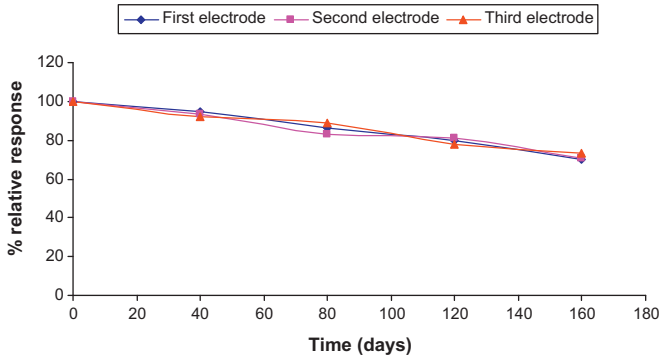

Fig. 9. Effect of storage at 4 °C on the response of three similar SO_x/PBNPs/PPY/ITO electrodes.

of variation were 2.2% and 4.3% respectively. The high precision indicated the good reproducibility and consistency of the present method. A comparison of sulfite values in 15 brands of red wine samples as measured by the present method (y) with those obtained by standard DTNB method (x) showed a good correlation with $r = 0.99$, regression equation being, $y = 0.9939 + 8.8496$ (Fig. 8). These results indicate the high accuracy of the method.

3.8. Interference study

The addition of the following interferrants such as ascorbic acid (4.8 μM), cysteine (0.24 μM), fructose (60 μM), glucose (22.2 μM), citric acid (100 μM), ethanol (70 μM) and glutamine (85 μM) evoked a negligible interference. A negligible interference was observed with these compounds (A decrease of only 4.08% for glutamine, 3.45% for glucose, 1.89% for citrate, 3.66% for fructose, 4.78% for cysteine and 2.85% for ascorbic acid on the biosensor response).

3.9. Application of biosensor for determination of sulfite in red and white wines

Sulfite level as measured by the present biosensor ranged from 175.8 to 416.8 μM in red wines and 375.7–720.4 μM in white wines (Table 1). These values are comparable to those stated in earlier reports [42]. Three similarly constructed enzyme electrodes were employed for determination of sulfite level in red wine samples in order to establish the reproducibility and variability of the present electrode. The results presented showed practically no significant variation (coefficient of variation less than 6% in all cases), confirming the reproducibility of present electrode.

3.10. Storage stability and reusability of biosensor

The electrode lost 30% of its initial activity after its 200 uses during the span of more than 3 months when stored at 4 °C, which is much better than earlier biosensors [23,24,27]. The results given in Fig. 9 show practically no variation in storage stability of the three electrodes.

A comparison of analytical characteristics of present sulfite biosensor with those of earlier amperometric biosensors is summarized in Table 2.

Table 1
Sulfite level in different brands of red and white wine samples as measured by SO_x/PBNPs/PPY/ITO electrode.

Samples	Sulfite level (μM) Mean ± SD[a] ($n = 4$)
1. Red wines	
(a) Grover La Reserva	416.8 ± 0.3
(b) Grover Cabernet Shiraz	333.5 ± 0.3
(c) Sula Cabernet Shiraz	235.7 ± 0.2
(d) Chantillit Shiraz	175.8 ± 0.3
(e) Sula Dindori Reserva	267.8 ± 0.2
(f) Chantillit Cabernet Sauvignon	318.5 ± 0.3
(g) Sula Satori Merlot	197.5 ± 0.3
2. White wines	
(a) Sula Chenin Blanc	720.4 ± 0.3
(b) Chantilli Chardonnay	664.5 ± 0.4
(c) Chantilli sauvignon Blanc	479.4 ± 0.2
(d) Sula sauvignon Blanc	375.7 ± 0.5
(e) Chantilli Chenin Blanc	597.2 ± 0.5

[a] Standard deviation.

Table 2
A comparison of analytical characteristics of present sulfite biosensor with those of earlier amperometric sulfite biosensors.

Properties	Dinckaya et al. [22]	Ameer and Adelozu [24]	Spricigo et al. [23]	Bahmani et al. [25]	Kalimuthu et al. [26]	Present
Support for immobilization	GC coated with thin Hg film	PPY	PASA modified Au electrode	Conducting PANI film	SAM of 11-mercaptoundecanol cast on Au electrode	PBNPs/PPY electrodeposited on ITO electrode
Method of immobilization	Crosslinking	Entrapment	Adsorption	Entrapment	Adsorption	Adsorption
Optimum pH	7	7	8.5	8.5	8	8.5
Optimum temp.	40 °C	ND	ND	35 °C	ND	35 °C
Response time	3 min	120 s	2 min	ND	3 s	2 s
Linearity (μM)	200–2800	0.9–400	*I*–60	6–500	1–6	0.5–1000
Detection limit (μM)	317	0.9	1	2	0.000044	0.12
Stability (days)	13	30	60	10	14	100

PPY, polypyrrole; PASA, polyaniline sulfonic acid; SAM, self assembled monolayer; PANI, polyaniline; PBNPs, prussian blue nanoparticles; ND, not detected.

4. Conclusion

The use of modified SO_x/PBNPs/PPY/ITO electrode has resulted into an improved analytical performance of the sulfite biosensor in terms of low response time (2 s), lower detection limit (0.12 μM) (S/N = 3), higher storage stability (100 days) and no interference by various interferrants compared to earlier biosensors. Based on these results, this composite could also be exploited for the improvement of analytical performance of other biosensors.

Appendix A. Supplementary data

Supplementary data associated with this article can be found, in the online version, at http://dx.doi.org/10.1016/j.ijbiomac.2012.06.008.

References

[1] A.Z. Ji, S.R. Savon, D.W. Jakobsen, Clinical Chemistry 41 (1995) 897–903.
[2] H. Kaziyama, Y. Nojima, H. Mitsuhashi, K. Urki, S. Tamura, T. Sekihara, U.R. Wakamats, S. Yano, T. Naruse, Journal of the American Society of Nephrology 11 (2000) 923–934.
[3] Federal Register, Food labeling: declaration of sulfiting agents 51,131 (1986a) 25012–25020.
[4] Federal Register, Sulfiting agents: revocation of gras status for use on fruits and vegetables intended to be sold raw to consumers 51,131 (1986) 25021–25026.
[5] A.I. Vogel, A Text Book of Quantitative Inorganic Analysis, fourth ed., ELBS, London, 1981.
[6] Y. Li, M. Zhao, Food Control 17 (2006) 975–980.
[7] M.R. Ceba, F.V. Jara, J.A.M. Leyva, Analyst 107 (1982) 781–786.
[8] M. Krishnamurty, N.V. Srinivasa Rao, Analyst 108 (1983) 119–122.
[9] M.D. Kester, P.M. Shiundu, A.P. Wade, Talanta 39 (1992) 299–312.
[10] T. Koh, K. Okabe, Analyst 119 (1994) 2457–2461.
[11] R. Von Wandruszka, X. Yuan, M.J. Morra, Talanta 40 (1993) 37–42.
[12] J. Hu, J. Zhu, I. Zhaeng, H. Gao, Fenxi Shiyanshi 13 (1994) 30–32.
[13] R.D. Rucklin, E.L. Johnson, Analytical Chemistry 55 (1983) 4–7.
[14] N. Kiba, M. Nishijma, M. Furusawa, Talanta 27 (1980) 1090–1092.
[15] J.L. Burguera, A. Townshend, Talanta 27 (1980) 309–314.
[16] J. Teckentrup, D. Klockow, Talanta 28 (1981) 653–663.
[17] D.K. Padma, Talanta 33 (1986) 550–552.
[18] I.K. Al-Hitti, G.J. Moody, J.D.R. Thomas, Analyst 108 (1983) 43–52.
[19] H. Hara, S. Okazai, Analyst 109 (1984) 1317–1320.
[20] J. Hengstenberg, B. Strum, O. Winkler, Messen Steuern und Regeln in der chemischen Technik, Band II, Springer-Verlag, Berlin, 1980.
[21] S. Theisen, R. Hansch, L. Kothe, R. Galensa, Biosensors and Bioelectronics 26 (2010) 175–181.
[22] E. Dinckaya, M.K. Sezginiturk, E. Akyilmaz, F.N. Ertas, Food Chemistry 101 (2007) 1540–1544.
[23] R. Spricigo, R. Dronov, F. Lisdat, S. Leimkühler, W. Frieder, U. Scheller, Analytical and Bioanalytical Chemistry 393 (2009) 225–233.
[24] Q. Ameer, S.B. Adeloju, Electroanalysis 20 (2008) 2549–2556.
[25] B. Bahmani, F. Moztarzadeh, R. Mohammad, T. Mohammadreza, Synthetic Metals 160 (2010) 2653–3265.
[26] P. Kalimuthu, J. Tkac, U. Kappler, J.J. Davis, P.V. Bernhardt, Analytical Chemistry 82 (2010) 7374–7379.
[27] R. Rawal, S. Chawla, T. Dahiya, C.S. Pundir, Analytical and Bioanalytical Chemistry 401 (2011) 2599–2608.
[28] X. Feng, Z. Sun, W. Hou, J.J. Zhu, Nanotechnology 18 (2007) 1–7.
[29] S. Wu, Y. Liu, J. Wu, H. Ju, Electrochemistry Communications 10 (2008) 397–401.
[30] J.C. Vidal, J. Espuelas, E. Garcia-Ruiz, J.R. Castillo, Talanta 64 (2004) 656–664.
[31] H. Zhao, Y. Yuan, S. Adeloju, G.G. Wallace, Analytica Chimica Acta 472 (2002) 113–121.
[32] R. Koncki, O.S. Wolfbeis, Biosensors and Bioelectronics 14 (1999) 87–92.
[33] A. Ahmad, A. Sarfraz, Indian Journal of Experimental Biology 48 (2010) 83–86.
[34] Satyapal, C.S. Pundir, Biochimica et Biophysica Acta 1161 (1993) 1–6.
[35] R. Bias, N. Potezny, J.B. Edward, A.M. Rofe, R.A.J. Conyer, Analytical Chemistry 52 (1980) 508–511.
[36] Y. Miao, J. Chen, X. Wu, Colloid Journal 69 (2007) 334–337.
[37] R. Devi, M. Thakur, C.S. Pundir, Biosensors and Bioelectronics 26 (2011) 3420–3426.
[38] J.J. Feng, G. Zhao, J.J. Xu, H.Y. Chen, Analytical Biochemistry 342 (2005) 280–285.
[39] A.K. Abass, J.P. Hart, D. Cowell, Sensors and Actuators B 62 (2000) 148–153.
[40] H. Mohammad, B. Baharak, M. Fatollah, R. Mohammad, Iranian Journal of Chemistry & Chemical Engineering 27 (2008) 115–121.
[41] H.K. Sezginturk, E. Dinckaya, Talanta 65 (2005) 998–1002.
[42] A.C. Isaac Livingstone, A.J. Wain, R.G. Compton, J. Davis, Trends in Analytical Chemistry 25 (2006) 589–598.